INSTITUT NATIONAL DES SCIENCES APPLIQUÉES TOULOUSE
Université Fédérale Toulouse Midi-Pyrénées
ONERA THE FRENCH AEROSPACE LAB
Département de Génie Mathématique & Modélisation

Projets tuteurés Recherche et Innovation

Flux uncertainty propagation on first-order traffic flow LWR model

May 24, 2023

Students :

Gorm	Finne Engelsen	
Pierre-Louis	Lemaire	INSA Toulouse - Department of Applied Mathematics
El Ghali	Berqoq El Alami	

Tutors :

Guillaume	Dufour	ONERA - Department of Information Processing and Modelling
François	Rogier	

Abstract :

There is an increasing need in society to regulate and better optimize traffic flows in our cities, with benefits ranging from reduced air pollution, increased safety, and independence from fossil fuels. For this purpose, scientists and engineers use different traffic flow models to measure the impact of various flow management measures, the Lighthill-Whitham-Richards (LWR) model being the best known. This paper deals with the propagation of flux uncertainties through the LWR model. We aim to show a comprehensive approach to quantifying the propagation of uncertainties from noisy input flux applied to the LWR model. It should be mentioned that the literature is vast regarding model optimization and the implementation and simulation of complex road networks. However, to this day, the study of uncertainty propagation remains poor because of the high computational costs. Using a Python solver developed by researchers from ONERA, we ran an uncertainty analysis with the Monte Carlo method and tracked vehicles travel times. Our results show that the noise does have an impact on the output of the LWR model but the propagation appears to be insignificant in comparison with the orders of magnitude of real situations.

Contents

Introduction **1**

1 LWR model **2**

1.1 Definition 2

1.2 Traffic Shock 3

1.2.1 Rankine-Hugoniot condition 4

1.3 The Fundamental Diagrams 4

2 Uncertainty Analysis **6**

2.1 Overview of the literature 6

2.2 Monte Carlo method for uncertainty analysis 6

2.2.1 Flux profiles, or traffic scenarios 7

3 Numerical investigations **8**

3.1 Solver 8

3.2 Simulations and workflow 8

3.2.1 Travel time computing 9

4 Results **10**

Conclusion **13**

Introduction

Motivation

The first attempt to model traffic flow goes back to 1934 when pioneer US-American Bruce D. Greenshields started studying traffic capacity [1]. However, the study of traffic flow has gained popularity in the past decades as science is challenged to find solutions to rising traffic while easy access to important computing power increases. Three main ways to describe traffic flow models has emerged in the literature, macroscopic, mesoscopic, and microscopic models [2]. We focus in this paper on macroscopic models, also known as "fluid" models, which is derived from a continuity equation (or transport equation) and a density-speed relation. One popular and unavoidable model in the literature is the Lighthill-Whitham-Richards (LWR) developed from the works of Lighthill and Whitham in 1955 and seperately by Richards in 1956 [3, 4]. Commonly used to model traffic flow, this model is based on the theory of hyperbolic partial differential equations (PDEs) and the assumption of a relationship between traffic flow and density. In order to achieve realistic and applicable results, scientists and engineers must be able to accurately model traffic flow in highly complex road networks. Readers can find examples of recent works that applied the LWR model to complex road networks here [5, 6, 7].

However, one may face major drawbacks when modeling traffic flow with the LWR model, as it being a macroscopic model, it does not take into account individual driver behavior, which is unpredictable and assumes a uniform driving population, while in reality in-homogeneity of drivers and vehicles can be relatively important. Such traffic dynamics rely heavily on the input data, which are prone to uncertainties in real applications. The models used can lead to the creation of shock waves, and their occurrence is completely defined by the initial and boundary conditions of the traffic. In an effort to prove the relevance of such a model to be used on a larger scale and applied to real-life problems, we must be able to quantify the propagation of uncertainties arising from real life measurements and identify the factors involved. We choose to focus on the study of the behavior of speed and density profiles when the input flux is subject to noise, and therefore measure how such uncertainties propagate on a road. Hence, we applied our investigations to multiple scenarios. We specifically paid attention to the sensibility to uncertainties of the model when appearing the creation of shock waves, i.e. traffic jams.

While the study of the application of the LWR model to complex networks and infrastructures has been extensively covered, uncertainty analysis remains rare in the literature [8]. This can be explained by the important numerical costs of running such analysis, mostly done through the Monte Carlo method. However, important computing powers have lately been easier to access, allowing us to proceed with such an investigation.

In this paper, we present our findings using a Monte Carlo (MC) approach to find an estimate of the propagation of uncertainties in the LWR model and their impact on the formation of traffic jams, as well as on the transit time experienced by users.

For readers that want to go further into this matter, recent findings for estimating the propagation of uncertainties generated by boundary conditions in transport equations have been proposed by O. Pannekoucke and his collaborators [9, 10]. Their approach is based on the use of Parametric Kalman Filters (PKF).

Outline of the paper

This paper is structured according to the following outline. In Section 1, we recall the concepts of the continuity equation, the LWR and the Greenshields models, and we also focus on the problem of shock waves. We detail our methodology for the uncertainty analysis, including our use of MC methods in Section 2. Before presenting the results, we clarify the methodology and tools used to proceed with our numerical investigation in Section 4. Results and conclusion are provided in Sections 3 and 4.

1 LWR model

1.1 Definition

The Lighthill-Whitham-Richards model is a macroscopic traffic flow model used to describe the behavior of vehicles on a road network. It was developed in the 1950s by three British mathematicians: Michael Lighthill, G. B. Whitham, and R. M. Richards [3, 4].

Before diving into the LWR model, let's focus on the basics and recall the fundamentals of the continuity equation. We observe, in Figure 1, a fluid traveling along the x-axis with a *flux* F.

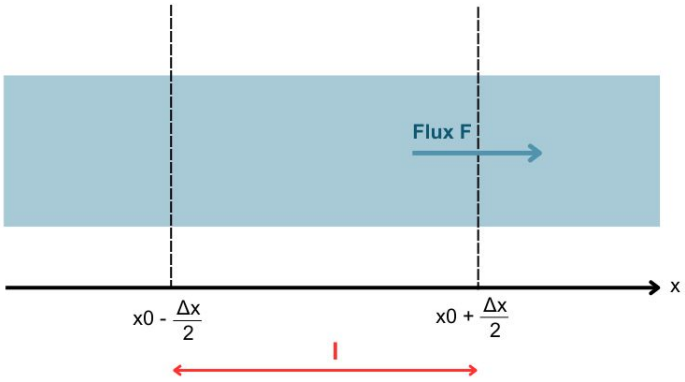

Figure 1: Conservation of the total number of vehicles on the interval I

We choose to focus on the space-interval $I = [x_0 - \frac{\Delta x}{2}, x_0 + \frac{\Delta x}{2}]$. With M the mass of the fluid and ρ its density:

$$M(t, x_0) = \int_I \rho(t, x)\, dx \tag{1}$$

We also observe that:

$$\lim_{\Delta x \to 0} \frac{M(t, x_0)}{dx} = \rho(t, x_0) \tag{2}$$

and,

$$\lim_{dt \to 0} \frac{\rho(t + dt, x_0) - \rho(t, x_0)}{dt} = \partial_t \rho(t, x_0) \tag{3}$$

Because of the conservation of the mass, it is equivalent to the *flux* entering from the left-side, minus the *flux* exiting at the right-side.

$$M(t + dt, x_0) - M(t, x_0) = -\int_t^{t+dt} F(s, x_0 + \frac{\Delta x}{2})\, ds + \int_t^{t+dt} F(s, x_0 - \frac{\Delta x}{2})\, ds \tag{4}$$

Following the same methodology for the $flux$ we obtain:

$$\lim_{dt \to 0} \frac{M(t + dt, x_0) - M(t, x_0)}{ds} = F(t, x_0 - \frac{\Delta x}{2}) - F(t, x_0 + \frac{\Delta x}{2}) \tag{5}$$

and therefore,

$$\lim_{\Delta x \to 0} \frac{F(t, x_0 - \frac{\Delta x}{2}) - F(t, x_0 + \frac{\Delta x}{2})}{dx} = \partial_x F(t, x_0) \tag{6}$$

We recall the continuity equation, implying the conservation of the mass of a fluid:

$$\partial_t \rho(t, x) + \partial_x F(t, x) = 0 \tag{7}$$

The LWR model states that traffic flow can be described as a "continuous" flow rather than individual cars. Hence, we represent the distribution of vehicles over a road section by a continuous density function $\rho \in \{\rho(t,x) : [0,\infty[\times\mathbb{R} \to \mathbb{R}, 0 \leq \rho \leq \rho_{max}\}$, and vehicles' speed by a density-dependent average speed $v \in \{v : \rho \to v(\rho), 0 \leq v \leq v_{max}\}$. Multiple speed-density relationships can be found in the literature [11], we chose to restrict our study to the simple linear Greenshields model that states:

$$v(\rho) = v_{max}(1 - \frac{\rho}{\rho_{max}}) \tag{8}$$

Treated as a fluid, traffic can experience changes in density, velocity, and pressure but also respects the Conservation Equation of Mass 1.1. Moreover, we know that $F(t,x) = \rho(t,x) \cdot v(t,x)$, thus comes the final equation of the LWR model:

$$\boxed{\frac{\partial \rho(x,t)}{\partial t} + \frac{\partial}{\partial x}(\rho(t,x)(v_{max}(1 - \frac{\rho(t,x)}{\rho_{max}})) = 0} \tag{9}$$

where x is the position, t the time, $v(t,x)$ the speed, $\rho(t,x)$ the traffic density and $\rho(t,x)v(t,x)$ the traffic flux as a function of density.

1.2 Traffic Shock

To simulate a traffic shock we choose the classic scenario where the traffic has come to a halt with an area of increased density. This means that incoming traffic meets traffic with higher density moving at a significantly slower velocity. Firstly by setting $v_{max} = 1$ and $\rho_{max} = 1$, and by some simplification in notation we obtain from 9 the following equation.

$$\rho_t + (\rho(1-\rho))_x = 0$$
$$\rho_t + (1-2\rho)\rho_x = 0$$

From this we get that the lines of characteristic are $\rho = c$ and $x = (1-2\rho)t + x_0$. Further, one can deduce that:

$$x'(0) = x_0 \qquad \phi(t) = \rho(t, x(t))$$
$$x'(t) = 1 - 2\rho(t, x(t)) = 1 - 2\rho_0(x_0) \qquad \phi'(t) = \partial_t\rho(t, x(t)) + x'(t)\partial_x\rho(t, x(t)) = 0$$

We then see that the change of position, x, in regards to t is linearly dependant on the density at the boundary condition, $\rho_0(x_0)$. Using the characteristic lines, we obtain Figure (2) showing how the shock occurs and using the equation for ρ above we get Figure (3).

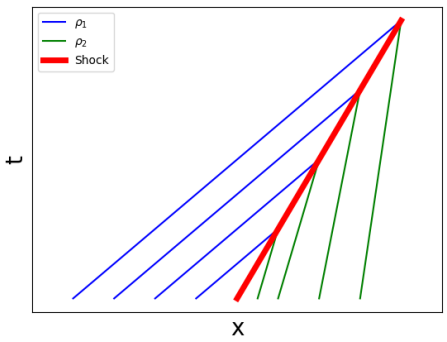

Figure 2: Creation of traffic shock as characteristic lines collide.

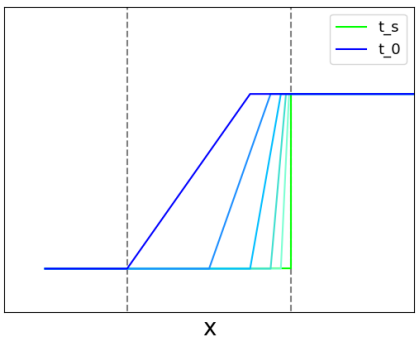

Figure 3: Creation of traffic shock as traffic moves

1.2.1 Rankine-Hugoniot condition

The Rankine-Hugoniot condition describes the relation between the two sides of a shock wave. It is based on the conservation of mass, momentum and energy. We firstly define the two different densities for before and after the shock wave, ρ_l and ρ_r, where the traffic at ρ_r is at a halt. We then define the rate of cars arriving at the shock as $F(\rho_l)$, while the rate of cars leaving the shock is $F(\rho_r)$. The speed of the shock is defined as s. The conservation of flow yields the following equation.

$$F(\rho_l) - F(\rho_r) = s(\rho_l - \rho_r)$$

Setting $\rho_r = 1$ we get the following expression for the speed of the shockwave.

$$s = \frac{F(\rho_l)}{\rho_l - 1}$$

This result is of interest when studying the propagation of error in situations with a shockwave.

1.3 The Fundamental Diagrams

Fundamental diagrams are graphical representations that show the relationship between traffic density, speed, and flow. These diagrams are useful for understanding the characteristics of road traffic and are used in traffic modeling to analyze traffic conditions, study road performance, and design efficient transportation systems.

The most commonly used fundamental diagram is the density-speed diagram. It represents the relationship between the density of vehicles on the road and the speed at which these vehicles are moving.

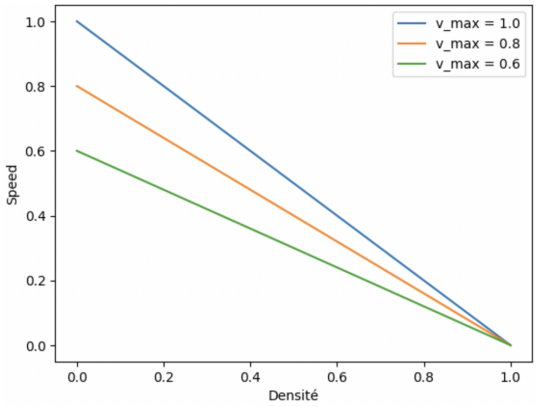

Figure 4: Speed-density fundamental diagram

It is observed that when traffic density is low, vehicles can travel at high speeds. However, as traffic density increases, speed decreases due to vehicle interactions. At a critical density, often referred to as the maximum density or congestion density, speed reaches zero.

The fundamental diagram can also be represented as a density-flow diagram, which shows the relationship between traffic density and traffic flow (the number of vehicles passing through a road section per unit time).

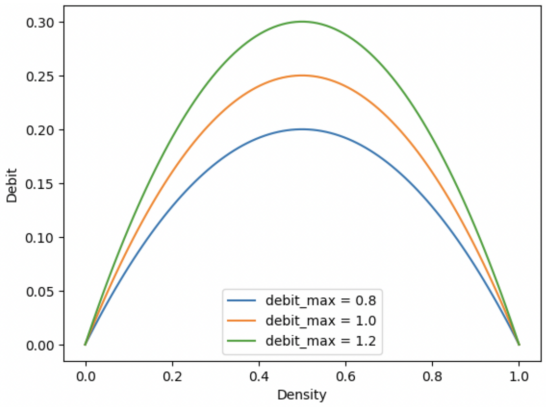

Figure 5: Flux-density fundamental diagram

It is observed that flow reaches a maximum at a specific density, known as the maximum flow density, and decreases at higher densities due to congestion effects.

In conclusion, these fundamental diagrams provide an intuitive graphical representation of the interactions between vehicles on the road and allow for the analysis of traffic performance. They are widely used in traffic modeling to assess traffic conditions, design efficient road infrastructures, and develop traffic improvement strategies. Therefore, while fundamental diagrams offer a solid foundation for understanding and analyzing traffic, they should be used with caution and complemented by other advanced techniques and models for a more accurate and comprehensive assessment of real traffic conditions.

2 Uncertainty Analysis

2.1 Overview of the literature

In order to clarify the framework of our analysis, we start by recalling a definition from the literature on uncertainty for system modeling: *"any deviation from the unachievable ideal of completely deterministic knowledge of the relevant system"* [12].

As discussed in the introduction and the previous section, macroscopic traffic flow models such as the LWR model don't fully characterize the reality of traffic flow dynamics that are subject to multiple disturbances, from infrastructure particularities, and unpredictable events, to individual behaviors of the chaotic order from vehicles. However, while it is undoubtedly true that such modeling will never be able to provide a full understanding and completely accurate forecasts of traffic flow, they are still commonly used by traffic and urban planners.

This accentuates the necessity to study the behavior of such models when subjected to parameter uncertainties, and, therefore, the need for thorough uncertainty analysis. In fact, risk and reliability assessments are considered a crucial part of most applicable engineering, from hydrology, civil engineering, structure mechanics, geotechnical engineering, etc [13].

In the fields of traffic models and, more generally, conservation laws, the literature already proposes multiple approaches to understanding these systems better. For example, the first-order LWR multi-class model's response to stochastic fundamental diagrams, *i.e.* varying flux over time, has been investigated [14], as well as another approach to solving general conservation laws with spatially varying flux functions using finite-volume methods [15]. While these papers do not directly deal with uncertainty analysis, studying the model's response to flux randomness falls into our uncertainty analysis framework.

As for the first-order LWR model, uncertainties mainly come from two sources. The solutions of the model originate from its fundamental diagram, which is supposed to represent the speed-density and flux-density relations observed in traffic over a stretch of road. Here we consider a linear and continuous relation, while in reality, the fundamental diagram rarely follows such restrictive assumptions. Moreover, measuring techniques are also subject to uncertainties, providing engineers and scientists with only an estimation of the traffic state. We accept the LWR model isn't a real-life model and choose to focus on the propagation of uncertainties arising from measurement errors, *i.e.,* a partial knowledge of the initial state, and of the incoming fluxes, which can be subject to noise. It is, relative to the literature described above, the main concern that faces such a model. We quantify these uncertainties through a simple Monte Carlo method, described in the following subsection.

Readers can investigate more sophisticated approaches to quantify such uncertainties, such as based on the Kalman Parametric Filters [9, 10], or the Polynomial Chaos (PC) methods [16]. We choose not to use these methods in this paper.

2.2 Monte Carlo method for uncertainty analysis

The Monte Carlo (MC) method is particularly efficient and simple to implement when estimating uncertainty propagation on the LWR model. This method consists of computing N_{mc} with a random parameter we call λ_{mc}. This parameter's randomness follows a specific distribution - we choose the *normal* distribution - therefore simulating noise. By applying this noise to our input *flux* function, over N_{mc} model iterations, we can simulate uncertainties and analyze the propagation of such noise in the LWR model output. Hence, the $flux$ function can be written as:

$$\tilde{f} = f + \lambda_{mc} f_c \tag{10}$$

with f the incoming $flux$ function at the entrance of the domain, $\lambda_{mc} \sim \mathcal{N}(0, \sigma^2)$ a random variable, and f_c a non-negative constant equal to 500 vehicles per hour.

2.2.1 Flux profiles, or traffic scenarios

Before computing the solutions, we must define multiple scenarios - or *flux* profiles - on which we will apply the noise defined above and then run the simulations. Details on the methodology and tools used for the numerical simulations are provided in Section 3. For this analysis, we define as follows, displayed in Figure 6, six *flux* profiles, representing typical traffic scenarios:

- **Reference scenario**: Input flux is constant and equal to the road flux. Numerical values will be detailed in Section 4.
- **Jump scenario**: Given an initial density ρ_{init}, we compute the compute the corresponding initial flux f_{init}. Then, for n_{jump} numerical iterations, we increase the input flux of df_{jump}, in order to reach $2 \cdot f_{init}$. Input flux then stays constant at this value. Preceding analysis of the LWR model indicate that this scenario does not create shock waves.
- **Drop scenario**: Given an initial density ρ_{init}, we compute the corresponding initial flux f_{init}. Then, for n_{drop} numerical iterations, we decrease the input flux of df_{drop}, in order to reach $0.4 \cdot f_{init}$. Input flux then stays constant at this value. As vehicles at higher density travel slower than vehicles at lower density, we should observe the creation of a shock wave.
- **Sinusoidal scenarios**: We choose n_{per} and compute a sinusoidal flux phased to start and end at the given flux, after going through n_{per} periods. For instance, we can decline the two preceding scenarios, *jump* and *drop*, to have sinusoidal forms.

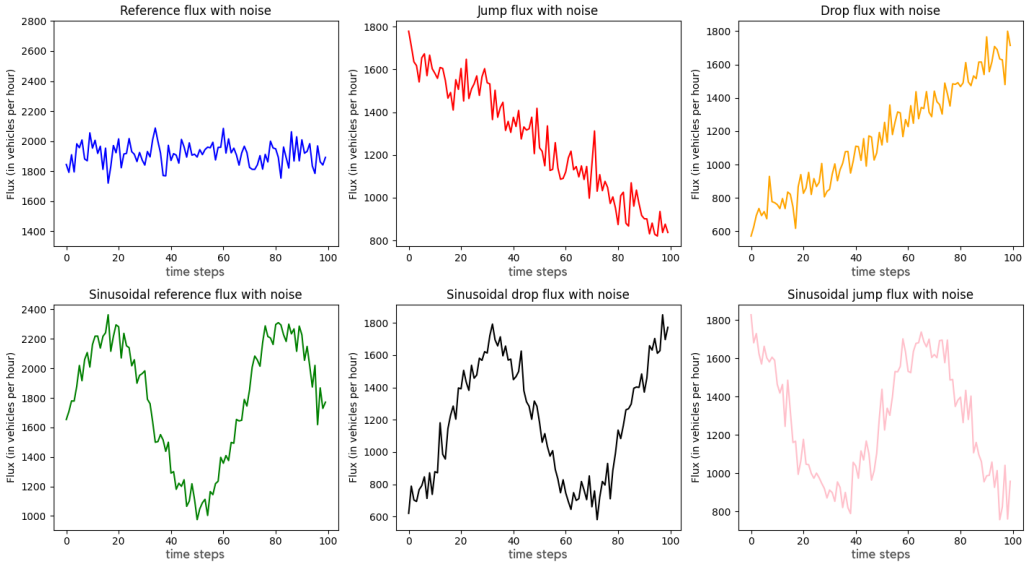

Figure 6: Flux profiles, with noise defined as above with $\sigma^2 = 0.15$

When running a simulation, we assign, at each time step to the model, an input flux corresponding to the scenario. Once the scenario is over, we assign the last flux value of the scenario as input flux, adding a random noise similar to the one of the scenario.

To study the impact of such noise on the output of the LWR model, and more generally, on traffic, we choose to focus principally on the travel time. We compute the travel time for a vehicle to go through the road once the scenario is over, for each flux scenario, with and without noise, and different values of σ^2. Travel time computing is detailed in Section 3.

3 Numerical investigations

3.1 Solver

As explained in Section 1.2, we deduce from the method of characteristics the equation which symbolizes the creation of a shock, *i.e.* a discontinuity in the density profile:

$$\partial_t \rho(t, x(t)) + F'(\rho(t, x(t)))\partial_x \rho(t, x(t)) = 0 \tag{11}$$

$$\Leftrightarrow \qquad \partial_t \rho(t, x(t)) + x'(t)\partial_x \rho(t, x(t)) = 0 \tag{12}$$

This can be characterized as a system of conservation laws. We also deduce an initial condition to add to our system:

$$\rho(t = 0, x(0)) = \begin{cases} \rho_{left}, & \text{if } x < 0 \\ \rho_{right}, & \text{if } x > 0 \end{cases} \tag{13}$$

Therefore, by combining our system of partial differential equations 12 and the initial condition defined above 13, we obtain what is called a Riemann problem. It is commonly recommended to use the Godunov scheme, which works as a finite volume method, for solving exact or approximate Riemann problems between each cell, as the domain is discretized.

To compute our simulations, we used a Python solver developed and provided by scientists from the research center ONERA (Office national d'études et de recherches aérospatiales), which implements the Godunov scheme to solve the Riemann problem explained above. As this is not the aim of the paper, we do not go any deeper into the technicality of the solver development.

3.2 Simulations and workflow

In this section, we explain our methodology for running simulations and studying uncertainty propagation. We start to generate an isolated road with classic parameters:

- **N**: the number of cells for road discretization.
- ρ_{init}: an initial density vector, of size similar to N. Values of ρ_{init} depend on the scenario we study, explained in Section 2.2.1.
- **I**: the number of lanes of the road.

Along with these parameters, we set classic LWR parameters, that stay constant for any scenario we want to run:

- ρ_{max}: the maximum density of vehicles that the road can support, in *vehicles per kilometer*.
- ρ_c: the critical density as in the Fundamental Diagram, explained in Section 1.3.
- V_0: the maximum speed allowed on the road, and ideally the vehicle's speed if $\rho = 0$, in *kilometers per hour*.
- **h**: the size of each mesh of the road, in kilometers.
- **dt**: the time step of the numerical scheme, in hours.

Once the framework of our study is established, we perform Monte Carlo simulations. For each scenario or flow profile described in Figure 6, we simulate $M = 200$ times our defined LWR model. Specifically, at each time step, the incoming flow of the road is noisy, according to the expression with a variance between 0.01 and 1, depending on the experiments. We also compute an output from a non-noisy flux to compare the results and better understand the uncertainties propagation.

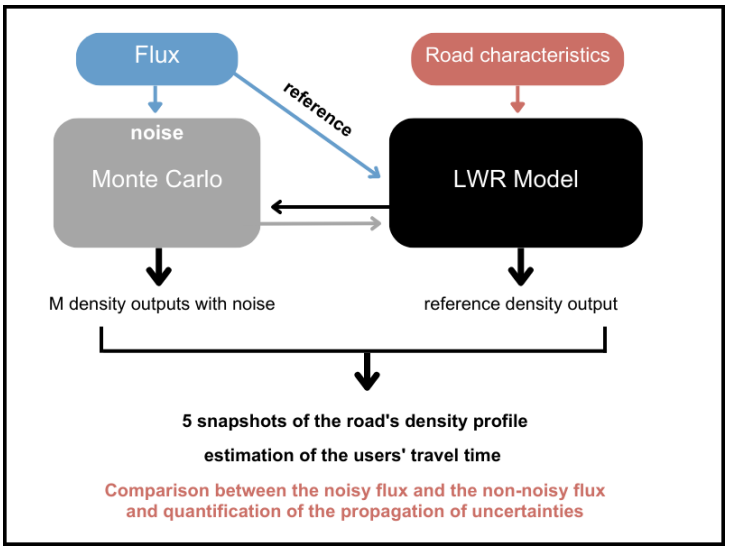

Figure 7: Monte Carlo uncertainty analysis workflow with LWR model

We recall our workflow in Figure 7. As explained in Section 2, we focus on the vehicles' travel time to quantify the impact of the flux uncertainties. We explain how we compute travel time in the next section.

3.2.1 Travel time computing

First, we set an iteration from which we will start to monitor the transit of the vehicle. For our analysis, we chose to start the monitoring once the "scenario" was passed. This means that if we choose to allocate 100 time steps to one scenario, let's say a *drop* in the density, we only start to compute the travel time of one vehicle at the 100^{th} iteration. Then, computing the travel time of the vehicle only means integrating the speed on the domain, *i.e.* the road.

4 Results

In this section, we present the results of our Monte Carlo analysis on the impact of input flux uncertainties on the first-order LWR model outputs. We remind the parameters of our numerical investigations:

- $N = 150$, the number of cells on the discretized road;
- $I = 1$, the road's number of lanes;
- $h = 0.1$ km, the length of the road's meshes;
- $dt = 0.001$ hour, the numerical scheme time step;
- $V_0 = 80$ km/h, the road's maximum speed;
- $\rho_{max} = 100$ vh/km, the road's maximum density.
- $\rho_c = 50$ vh/km, the road's critical density;
- $M = 200$ Monte Carlo iterations;
- $\sigma^2 \in [0.01, 0.15, 0.3, 0.5, 1.0]$ the variance of the noise (see Equation 10).

We refer readers to Section 3 for more details on the above parameters, as well as for the six flow scenarios on which we will run the LWR model. First, we can observe in Figure 8 the behavior of the LWR model when the input flux is non-noisy.

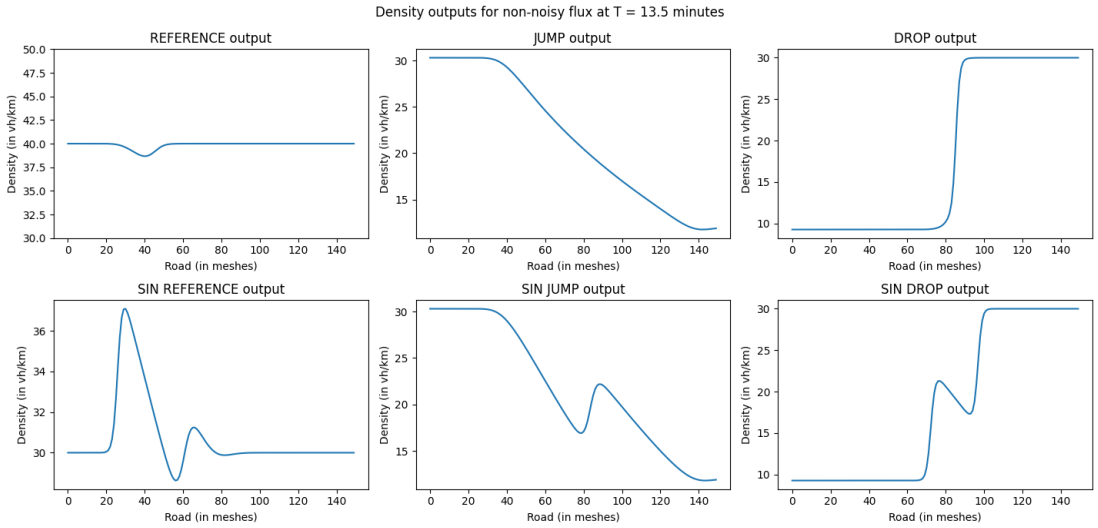

Figure 8: Density outputs for non-noisy flux at T = 13.5 minutes

Because of the speed-density fundamental diagram of the LWR model (see Figure 4), the higher the density at a given x position on the road, the lower the vehicles' speed will be at this position. Meaning that vehicles on a high-density portion of the road will travel slower that vehicles on a low-density position of the road. This explains the output of the *jump* scenario, as vehicles on the right side of scenario (low-density) will travel faster than vehicles on the left-side of the scenario (hihg-density), creating this continuous slope that doesn't lead to any shock. While for the *scenario*, vehicles from the left-side travel faster than vehicles from the right-side, making the upper bound of the density profile moves slower than the lower bound, leading to a shock wave, or also called traffic-jam.

As explained in Section 1.2, by the method of the characteristics, we can explain mathematically why the *drop* scenario will create a shock wave, whereas the *jump* scenario will not lead to any shock. We recall the equation of the characteristics:

$$x'(t) = 1 - 2\rho_0(x_0) \tag{14}$$

the general initial conditions for a *drop* scenario (on the left) and for a *jump* scenario (on the right),

$$\rho_0(x) = \begin{cases} 0, & \text{if } x < 0 \\ 1, & \text{if } x > 1 \\ x, & \text{else} \end{cases} \qquad \rho_0(x) = \begin{cases} 1, & \text{if } x < 0 \\ 0, & \text{if } x > 1 \\ 1 - x, & \text{else} \end{cases} \tag{15}$$

Figures 9 and 10 show the characteristics diagrams of each of these scenarios. We point out to the readers, that we do not in fact observe any intersection of the characteristics in Figure 10, while we observe an intersection at $t = 1/2$ in Figure 9.

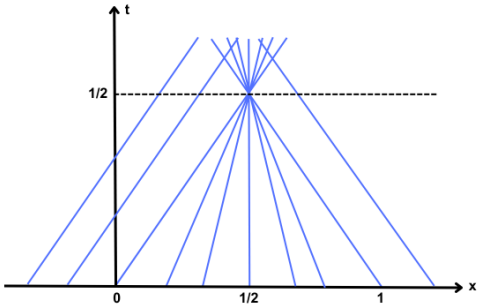

Figure 9: Characteristics diagram for the *shock* initial conditions

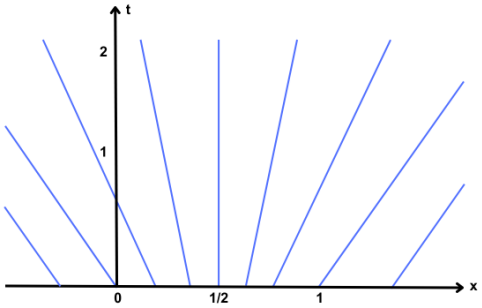

Figure 10: Characteristics diagram for the *jump* initial conditions

When running Monte Carlo simulations (with $M = 200$) with noisy-flux (setting $\sigma^2 = 0.5$), we observe no significant difference compared to the non-noisy flux outputs for any value of $\mathbf{T}$. We illustrate this statement by Figure 11 below.

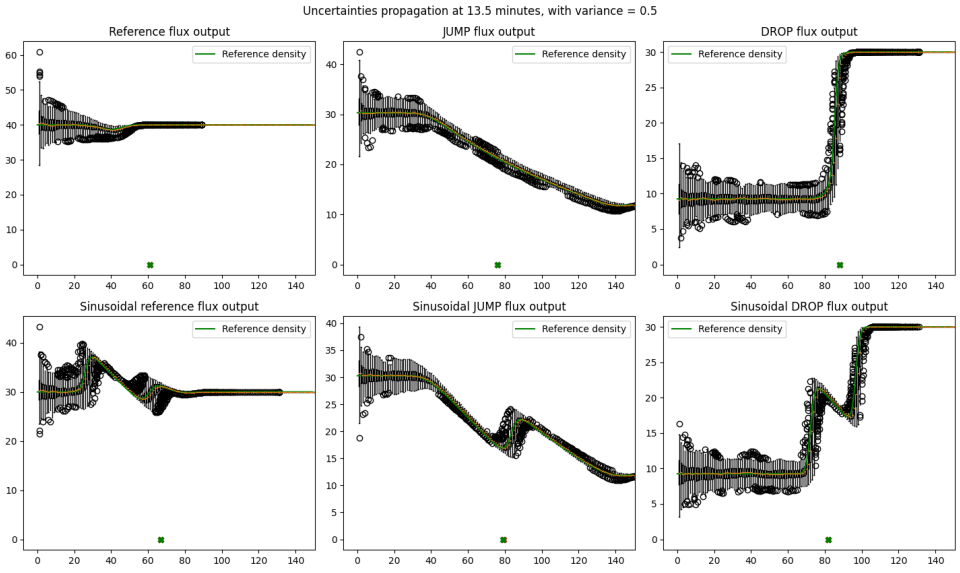

Figure 11: Density profiles at T = 13.5 minutes for $\sigma^2 = 0.5$

This observation seems to be confirmed by the average values of travel times, regardless of the flux scenario. We have compiled in Figure 12 the average travel times for each scenario, differentiating between a simulation with noisy and non-noisy input flux.

Variance	0.01		0.15		0.3		0.5		1.	
Flux scenario	with noise	without noise	with noise	without noise	with noise	without noise	with noise	without noise	with noise	without noise
REFERENCE	24.54	24.54	24.53	24.54	20.54	20.54	24.53	25.54	24.47	24.54
JUMP	20.34	20.34	20.36	20.34	20.36	20.34	20.36	20.34	20.37	20.34
DROP	20.04	20.04	20.03	20.04	20.02	20.04	20.02	20.04	20.00	20.04
SIN REFERENCE	22.32	22.32	22.32	22.32	22.32	22.32	22.34	22.32	21.90	22.32
SIN JUMP	20.04	20.04	20.04	20.04	20.04	20.04	20.05	20.04	20.03	20.04
SIN DROP	20.04	20.04	20.03	20.04	20.02	20.04	20.02	20.04	20.05	20.04

Figure 12: Travel times for each flux scenarios, **in minutes**

We observe no significant change due to the noise added to the input flux. In fact, there is no difference between the noisy and non-noisy flux for the *reference* and *sinusoidal reference* scenarios.

However, both the *drop* and the *sinusoidal drop* scenarios react with faster travel times with noisy flux. For $\sigma^2 = 0.5$, we observe a 0.1% **decrease** in travel time. We observe a 0.09% **increase** in travel time for the *jump* scenario. Still, as we can observe in Figure 11, the impact of the noise is insignificant, as the green cross, representing the vehicle location for the non-noisy flux, is indistinguishable from the red cross, which represents the location of the vehicle location for the noisy-flux, whatever the scenario.

We do not comment on our results for $\sigma^2 = 1.0$ as the results show no real tendencies. This is due to the low number of M Monte Carlo iterations. Because of the numeral cost of such analysis, we couldn't run other simulations with higher MC iterations.

One can wonder if noisy flux impact the travel times distributions. Figure 13 shows that travel time variances remain low compared to the noise. However, we note that there is a surlinear relationship between the noise variance and the travel time variance. *Jump* fluxes also seem to present higher travel time variances than other flux scenarios. When compared to the noise relative standard deviation, as in Figure 14, the travel time RSD remains small (around 2% of the noise RSD). This means that the noise doesn't have an impactful effect on the traffic conditions.

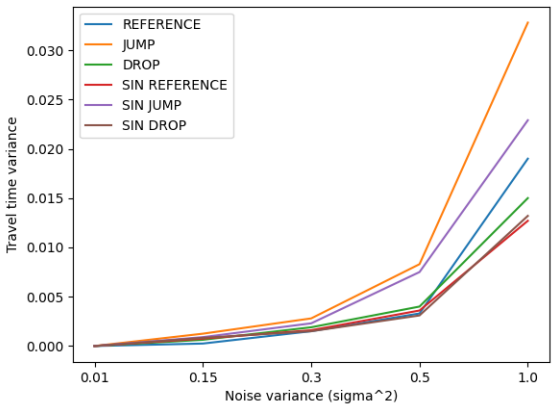

Figure 13: Characteristics diagram for the *shock* initial conditions

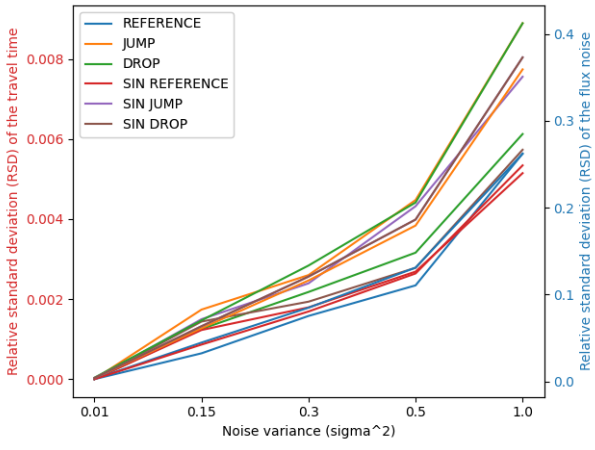

Figure 14: Relative standard deviation of the flux noise and travel times for each scenario

Conclusion

This paper focused on quantifying the impact of input flux uncertainties on the first-order LWR model outputs through a Monte Carlo analysis. We use a Python solver developed by scientists from ONERA to run simulations on the LWR model.

The Monte Carlo method was chosen as an efficient and simple approach to estimate uncertainty propagation in the LWR model. We simulated noise and applied it on the model input fluxes thanks to a random variable following a normal distribution. Then we examined different flux scenarios and compared the travel times for simulations with and without noisy input flux. The results indicated that noisy flux do not lead to significant different outputs than non-noisy flux, for all the flux scenarios we tested. It can be deduced from this result that in a more complex road network, uncertainties do not propagate, From this result, it can be deduced that in a more complex road network, uncertainties do not propagate - on a scale that would require intervention - from road to road.

The impact of the noise on the density profiles was also studied through snapshots of the density vectors. The research emphasized the importance of uncertainty analysis in macroscopic traffic flow models like the LWR model, considering the multiple disturbances and uncertainties present in real traffic flow dynamics. While the LWR model may not fully capture the complexity of traffic flow, it remains commonly used in traffic and urban planning. Therefore, understanding the behavior of such models under parameter uncertainties is crucial. The research highlighted the need for thorough uncertainty analysis and referred to existing approaches in the literature.

In conclusion, this research project provided insights into the propagation of input flux uncertainties in the first-order LWR model. While we achieved satisfying results in relation to this paper objectives, we recommend to continue investigating this subject with more sophisticated approach (readers can refer to [10, 9, 16]) or with more computational power to push the Monte Carlo analysis further, by performing more iterations (a suitable number would be 10000). The findings contribute to the understanding of uncertainty in traffic models and can inform future studies and applications in traffic and urban planning.

We would like to especially thank Guillaume DUFOUR, researcher at ONERA Toulouse, for his implication in this project, his trust, and his precious help guiding us through our research. A special thank you to Joseph SHEA who personally supervised the editorial quality of this paper.

References

[1] B. D. Greenshields, "A study of traffic capacity," *Highway Research Board Proceedings*, vol. 14, pp. 448–477, 1935. [Online]. Available: https://trid.trb.org/view/120649

[2] M. Treiber and A. Kesting, "Traffic flow dynamics," pp. 55,65, 2013. [Online]. Available: https://link.springer.com/book/10.1007/978-3-642-32460-4

[3] M. Lighthill and G. Whitham, "On kinematic waves. i: Flood movement in long rivers. ii: A theory of traffic flow on long crowded roads," *Proceedings of the Royal Society*, pp. 281,345, 1955.

[4] P. I. Richards, "Shock waves on the highway," *Operations Research*, vol. 4, pp. 42,51, 1956. [Online]. Available: https://pubsonline.informs.org/doi/10.1287/opre.4.1.42

[5] G. Coclite, M. Garavello, and B. Piccoli, "Traffic flow on a road network," *SIAM J. Math. Analysis*, vol. 36, pp. 1862–1886, 01 2005. [Online]. Available: https://www.researchgate.net/publication/220132206_Traffic_Flow_on_a_Road_Network

[6] M. Garavello and B. Piccoli, "Traffic flow on a road network using the aw–rascle model," *Communications in Partial Differential Equations*, vol. 31, no. 2, pp. 243–275, 2006. [Online]. Available: https://doi.org/10.1080/03605300500358053

[7] Y. Chitour and B. Piccoli, "Traffic circles and timing of traffic lights for cars flow," *Discrete and Continuous Dynamical Systems - B*, vol. 5, no. 3, pp. 599–630, 2005. [Online]. Available: https://www.researchgate.net/publication/224010782_Traffic_circles_and_timing_of_traffic_lights_for_cars_flow

[8] J. Li, Q.-Y. Chen, H. Wang, and D. Ni, "Analysis of lwr model with fundamental diagram subject to uncertainties," *Transportmetrica*, vol. 8, 2011. [Online]. Available: https://www.researchgate.net/publication/228345307_Analysis_of_LWR_model_with_fundamental_diagram_subject_to_uncertainties

[9] O. Pannekoucke, R. Ménard, M. El Aabaribaoune, and M. Plu, "A methodology to obtain model-error covariances due to the discretization scheme from the parametric kalman filter perspective," *Nonlinear Processes in Geophysics*, vol. 28, no. 1, pp. 1–22, 2021. [Online]. Available: https://npg.copernicus.org/articles/28/1/2021/

[10] M. Sabathier, O. Pannekoucke, V. Maget, and N. Dahmen, "Boundary conditions for the parametric kalman filter forecast submited," 2022. [Online]. Available: https://arxiv.org/abs/2212.10921

[11] P. Rai, "A study of hyperbolic traffic flow models," *Département des Mathématiques Appliquées et Calcul Intensif (MACI), ONERA*, 2022.

[12] W. Walker, P. Harremoës, J. Rotmans, J. van der Sluijs, M. van Asselt, P. Janssen, and M. K. von Krauss, "Defining uncertainty: A conceptual basis for uncertainty management in model-based decision support," *Integrated Assessment*, vol. 4, no. 1, pp. 5–17, 2003. [Online]. Available: https://doi.org/10.1076/iaij.4.1.5.16466

[13] H. Garg and M. Ram, *Engineering Reliability and Risk Assessment*, 2023. [Online]. Available: https://doi.org/10.1016/C2020-0-04541-X

[14] D. Ngoduy, "Multiclass first-order traffic model using stochastic fundamental diagrams," *Transportmetrica*, 2011. [Online]. Available: http://dx.doi.org/10.1080/18128600903251334

[15] D. S. BALE, R. J. LEVEQUE, S. MITRAN, and J. A. ROSSMANITH, "A wave propagation method for conservation laws and balance laws with spatially varying flux functions," *SIAM*, vol. 24, no. 3, pp. 955, 978, 2002. [Online]. Available: https://faculty.washington.edu/rjl/pubs/vcflux/39738.pdf

[16] G. Poëtte, B. Després, and L. Didier, "Uncertainty quantification for systems of conservation laws," *Journal of Computational Physics*, vol. 228, no. 7, pp. 2443, 2467, 2009. [Online]. Available: https://doi.org/10.1016/j.jcp.2008.12.018